atmosphere

MDPI

Article

A Simple Conceptual Model for the Heat Induced Circulation over Northern South America and Meso-America

Julián David Rojo Hernández * and Óscar José Mesa

Departamento de Geociencias y Medio Ambiente, Facultad de Minas, Universidad Nacional de Colombia, Carrera 80 No 65-223, Bloque M2-316, Medellín 050041, Colombia; ojmesa@unal.edu.co

* Correspondence: jdrojoh@unal.edu.co; Tel.: +57-3117397113

Received: 23 October 2020; Accepted: 11 November 2020; Published: 17 November 2020

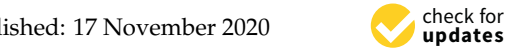

Abstract: The physical description of the atmosphere's general circulation over Northern South America and Meso-America deserves a more comprehensive explanation. This work presents the Pacific coast of Colombia as the rainiest place on Earth, with annual rainfall averaging 5000 to 13,000 mm, and record values as high as 13,159 mm for the location of Puerto López (77°14′ W, 2°50′ N). Using information from the ECMWF ERA-40 Atlas and ERA-Interim Reanalysis, we describe the existence of a concentrated diabatic heating source due to condensation and the main features of its related circulation over Northern South America and Meso-America. For simplicity, we used the analytical solution of the Phlips-Gill Model to diagnose the main flow patterns. Results show that the diabatic source over western Colombia generates equatorial trapped Rossby-Kelvin waves, which dominate the low-level circulation. A Kelvin wave explains the low-level easterly flows over the Tropical Atlantic Ocean, the Caribbean Sea, the Venezuelan-Colombian Llanos, and the Northern Amazon Basin. This circulation is analogous to a Walker cell. To the west, two cyclonic flows and strong westerly winds are present in Meso-America and the far eastern Pacific because planetary waves propagate there. A slight asymmetry in the equator's diabatic heating location is responsible for the intense low-level pressure over Panama. The vertical velocity over the source area induces vortex tube stretching, and zonal mean flow excites a mixed wave and a northward flow.

Keywords: Matsuno-Gill model; Northern South America circulation; Rossby-Kelvin waves; Walker circulation; low level jets

1. Introduction

Despite some advances, there is no satisfactory theory explaining the main circulation patterns in northern South America and Meso-America. This region exhibits some notorious meteorological features, including persistent deep atmospheric convection, unusually high rainfall over western Colombia, and the far East Pacific. A better understanding of this region's circulation will advance western hemisphere tropical meteorology and climatology.

The region covers the tropical Americas (15° S–15° N, and 30° W–100° W) encompassing Central America, Colombia, Venezuela, Ecuador, Peru, and northern Brazil, as is shown in Figure 1. It includes the tropical North Atlantic and tropical South Atlantic Ocean, the Caribbean Sea, and the eastern tropical Pacific Ocean. Regional atmospheric circulation and climate arise from interactions with the neighboring oceans, the Andes and the Guiana Shield, the mountains of Central America, the Venezuelan–Colombian Llanos, and the Amazon basin. The work of [1] provides an excellent initial review of regional climatology, Refs [2,3] presented most of the main pathways of local circulation.

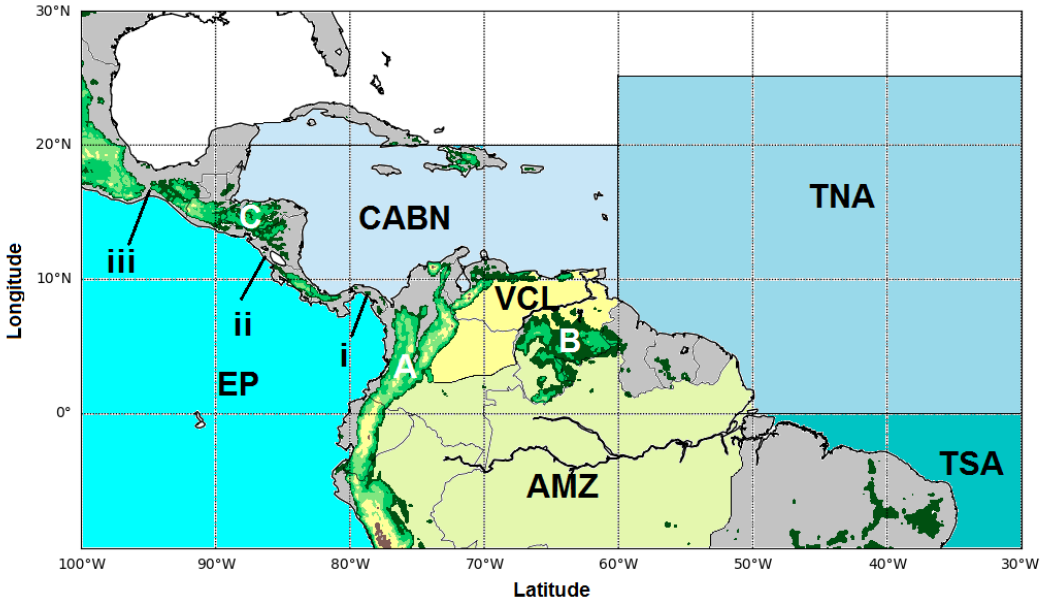

Figure 1. Map of northern South America and Meso-America depicting the regions used in the description of the circulation. Mountain ranges: (**A**) The Andes, (**B**) Guiana Shield, (**C**) Mountains of Central America. Oceans: *TNA* Tropical North Atlantic, *TSA* Tropical South Atlantic, *CABN* Caribbean Sea, *EP* Estern Pacific. Isthmus: (**i**) Panama, (**ii**) Papagayo, (**iii**) Tehuantepec. Regions: *VCL* Venezuelan-Colombian Llanos, *AMZ* Amazon basin.

1.1. The Rainiest Place on Earth

Table 1 presents the annual average precipitation and the total yearly maximum rainfall for some stations located on the Pacific coast of Colombia using the official data of the Institute of Hydrology Meteorology and Environmental Studies (IDEAM). Table 1 also gives the first year of records and the geographic coordinates of each station. Figure 2a shows areas with precipitation above 4000 mm/year; most of the low-level lands in western Colombia receives more than 6000 mm/year. López de Micay rain gauge station (77°14′ W, 2°50′ N), with 13,159 mm/year of mean annual rainfall (1960–2018) probably is the rainiest place on Earth. In the neighborhood, there is another gauge, San Antonio de Yurumangui (77°15′ W, 3°15′ N) that in 2018 recorded an annual rainfall of 26,987 mm. Both records surpass Lloró [4], Cherrapunji, India, and Mr. Waileale's, Hawaii, widely accepted as the rainiest locations on Earth [5] (p. 355).

Table 1. Mean annual rainfall and maximum annual record values at diverse gauging stations in western Colombia.

Station	First Year	Lat.	Lon.	P Mean mm/Year	P Max mm/Year
Pto López	1960	2.85	−77.25	13,159	22,572
Concha La	1985	3.17	−77.14	12,069	20,288
Tutunendo	1966	5.74	−76.54	10,946	19,468
Yurumangui	1980	3.26	−77.26	10,536	26,987
Junín	1963	1.34	−78.12	9106	12,125
Nóvita	1966	4.96	−76.61	9020	13,763
Vuelta la	1943	5.46	−76.55	8741	11,522
Bebedó	1973	4.93	−76.83	8724	13,551
Cértegui	1967	5.38	−76.61	8264	11,522
Lloró	1983	5.50	−76.54	8240	10,695
Apto El Carano	1947	5.69	−76.64	8128	12,182
Opogodó	1966	5.06	−76.65	8029	14,157

1.2. A Strong Diabatic Heating Source

Rain is the driving force of the atmospheric tropical circulation by releasing latent heat. Besides, the convergence of moist air in the lower atmosphere fuels convection [6]. Equatorial waves play an essential role in this mutual interdependence between rain and convergence. Ref [7] studied the thermodynamic structure of the atmosphere using the vertically integrated diabatic heat from ERA-40 and NCEP reanalyses, employing the residual diagnosis of the thermodynamic equation. Their results confirmed that, from mid-March to mid-December, over northern South America, specifically in western Colombia, there is one of the most prominent diabatic heating regions on Earth. The area of diabatic heating is relatively small in extent. These observations are also consistent with the dynamics of the outgoing longwave radiation in the region [8].

Figure 2b shows the annual mean column-integrated diabatic heating over Meso-America and South America. There is a robust diabatic heating source over western Colombia. Annually, it is the second-largest on Earth with a magnitude 815 W/m^2, but the seasonal analysis of ERA-40 Atlas shows that it is the strongest one during fall (September, October, November). Another diabatic heating source sits in the Andes' eastern flank over Peru and Bolivia around 15° S. The same seasonal analysis demonstrates that it is relevant only during boreal winter (December, January, February).

1.3. Far Eastern Pacific Cyclonic Vortexes

Other notorious features are two persistent cyclonic vortexes on the western side of this diabatic heating source. During most of the year, one can observe how the winds coming from the Caribbean sea recurve towards the south, crossing Panama, Papagayo, and Tehuantepec isthmus [9], and then turn to the west to reach the Colombian coast [2]. This recurving seems stronger than another one coming from the south, referred to as CHOCO jet [4]. The corresponding change in the sign of the Coriolis acceleration for the cross-equatorial winds, the predominant north-south coast orientation, the land-sea temperature gradient, and the friction gradients could contribute to establishing a westerly jet at $5^{\circ}N$; for those reasons, the traditional CHOCO jet explanation so far is the Stensrud mechanisms [10]. Finally, moisture advection associated with the related circulation produces copious orographic precipitation in the Andes' western flank.

Figure 2c presents a review of the general circulation in the low troposphere by drawing the streamlines of the multi-annual mean wind fields of the ERA-Interim Reanalysis. This Figure shows two cyclones, the first one over Panama and the other slightly weaker on the equator. Together, those cyclones generate strong westerly winds around 5° N in the far eastern Pacific ocean. The most prominent vertical velocity locates over the heating area. As shown in Figure 2d, in the upper troposphere, two anticyclones are evident, the first over Meso-America and the second over the Bolivian and Peruvian plateau (referred to as Bolivian High). The first one is responsible for strong easterly winds to the west side of the diabatic heating source and westerlies to the east.

1.4. The Atlantic—South America Walker Circulation

The term Walker's circulation [11] has come to be applied not just to the equatorial zonal circulation over the entire Pacific but also to that of the other equatorial zonal flows across the Atlantic and Indian Oceans as well ([12–15]).

Mainly, the Walker circulation and its zonal structure arise as a natural response to the equatorial heating concentrated in the western portions of the Pacific, Atlantic, and Indian ocean basins [16,17]. Atmospheric heating comes mostly from the latent heat release associated with deep, moist convection in the associated moist, unstable environments. Among the essential contributions to deep moist convection are the upslope flows on the western side of Africa's mountain ranges, northern South America, and Asia [6].

Wang studied the Walker cell Circulation between the tropical Atlantic sea and Northern South America ([18,19]). This Walker cell is responsible for easterly winds from the Atlantic ocean to Northern

South America and the far eastern Pacific. At the same time, the air rising over Colombia is part of the cell.

Figure 2e presents a vertical profile at around 5° N and displays the Walker circulation between the tropical Atlantic Ocean and Northern South America. Low-level easterly winds travel from the tropical Atlantic Ocean to the Venezuelan-Colombian Llanos, the Guiana Shield, and the northern Amazon rainforest and then raise in the Andes to return to the west in the upper atmosphere (300 hPa).

1.5. The Central Hypothesis of This Work

From the above review, it is clear that there is intense diabatic heating concentrated over western Colombia. This heating source's existence is due to the convergence of low-level moisture toward the Andes, which produces large amounts of orographic precipitation and the consequent large amount of latent heat release from the beginning of March until the end of November. On the west side of the heating source, two cyclonic circulations are responsible for strong westerly winds, the first in the northwest branch associated with the Caribbean jet, the second in the southwest. These westerly winds produce the low-level CHOCÓ jet. On the east side of the heating source, easterly winds go from the tropical Atlantic to northern South America, traveling parallel to the equator as a part of a Walker circulation. Notoriously, the most substantial vertical velocity is over the diabatic heating source.

Multilevel models and even full atmospheric general circulation models (AGCMs) could be used to compute responses to heating with greater generality, but their complexity makes it challenging to gain insight into fundamental processes. There are several models of heat-induced circulation founded on early work by [20,21] whose basis, in turn, come from the previous work on linear equatorial wave theory [22]. Those models' main assumptions are (i) diabatic heating in deep convection drives the surface winds, and (ii) linear dynamics is adequate to understand the surface wind response to this heating.

Webster and Gill also found a significant asymmetry in the circulation at the east and west side of the heat source explained by solutions of the shallow waters equations in steady-state with a forcing equivalent to a concentrated heating source. The Kelvin waves' full structure explains the Walker circulation with easterly near-surface trade winds flowing parallel to the equator, accelerating toward the heating source and subsequently rising through the heat source before flowing eastward aloft. On the other hand, planetary waves describe that two cyclones are responsible for the re-curvature of the circulation and the establishment of westerly winds on the western side of the heating source. These damped baroclinic Rossby-Kelvin pattern depicted by the Matsuno–Gill model are the cornerstones for our understanding of heat-induced atmospheric circulations in the tropics.

Diabatic heating associated with tropical precipitation drives a local response in the regional atmospheric circulation, but there is also excitation of equatorial waves. These equatorial waves induce a remote reaction and a large scale circulation [23]. Thus, the diabatic heating's three-dimensional structure closely relates to the atmospheric circulation because it drives the flow distribution and receives feedback. It is not easy to find a work that shows the main features of northern South America and Mesoamerica circulation into a simple theory regarding the main elements of low latitudes dynamics (Condensation heating, equatorially trapped waves, and large scale circulation). Most of the literature considers the main features of general circulation over this region as isolating mechanisms. There is an open debate about the real causes and consequences of deep convection in this part of the globe.

Given this background, we considered using the Matsuno-Gill model because it is perhaps the simplest dynamic model for the heat-induced tropical circulation. For this purpose, we perform the analytical solutions provided by the Phlips and Gill framework [24], which allows a response for different heating sources geometries and locations in terms of the natural modes, planetary, Kelvin, and gravity-planetary waves. The paper proceeds with some analytics experiments to reproduce the main flow features of regional circulation, including a heating area north of the equator and a wind ambient influence in a non-resting case. The Rossby-Kelvin pattern of the Matsuno-Gill model and

documented observations about the atmosphere's general circulation over northern South America and Meso-America are consistent with supporting the statement that a set of trapped waves in the tropics induced by a heating source explain the flow over this region.

1.6. The Organization of the Paper

Section 2 explains how the main features of the regional circulation arising from the diabatic heating due to intense precipitation fit with the description in the literature review. This correspondence justifies our proposal that the circulation is arising from exited equatorially trapped waves. We also compare Reanalysis with the simple model results. Section 3 discusses the model and how it describes the main features of the circulation. Section 4 describes data and methods.

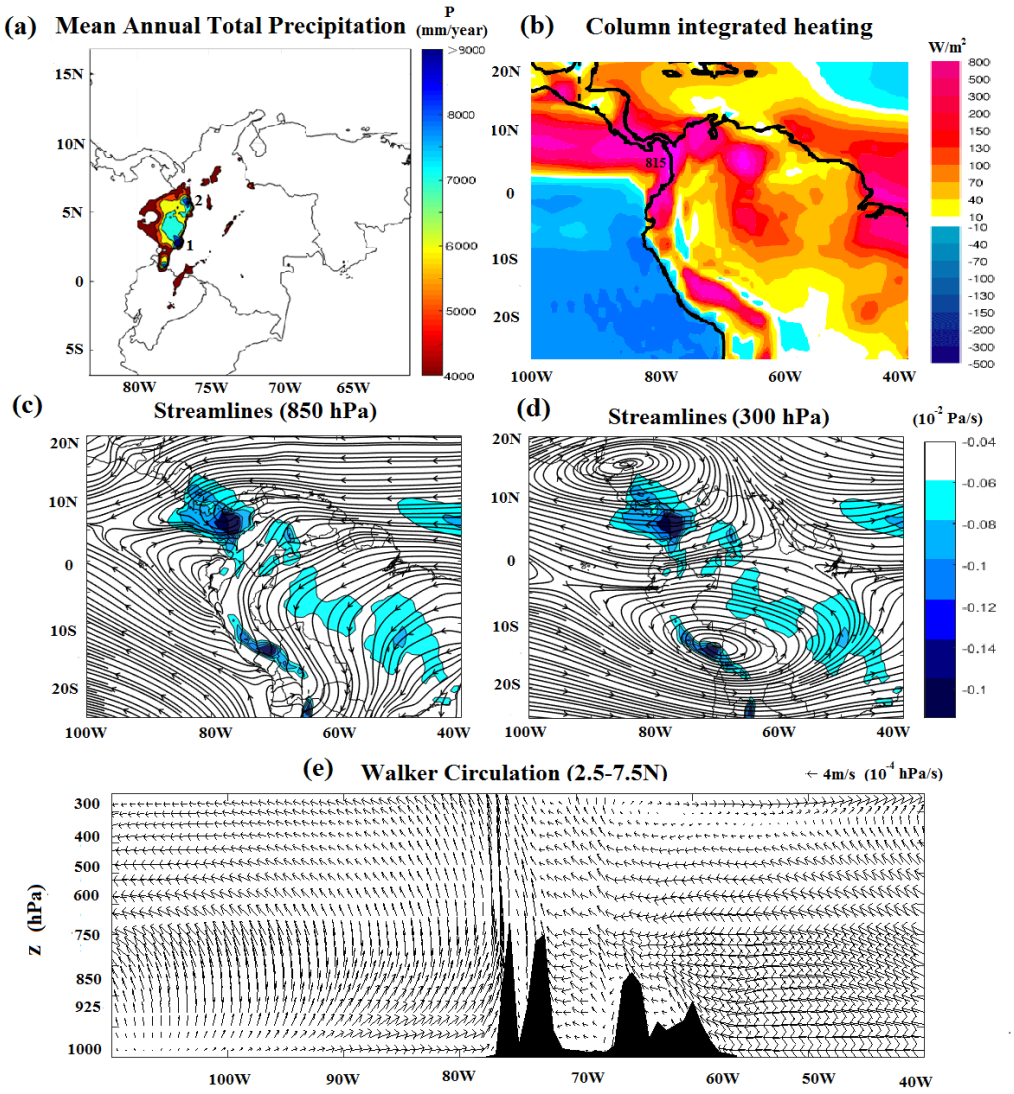

Figure 2. Average multiannual circulation in northern South America (**a**) Regions with precipitation above 4000 mm computed from Hurtado-Montoya and Mesa [25]. (**b**) Total column vertically integrated diabatic heating from ERA-40 Atlas [26]. (**c**) Streamlines at 850 hPa (**d**) Streamlines at 300 hPa. (**e**) Vertical cross section depicting the Walker circulation, taken from ERA-Interim Reanalysis.

2. Results

2.1. Main Flow Patterns over Northern South America and Mesoamerica

Figure 3 shows the Phlips and Gill solution for equatorially symmetrical heating located at 77° W. One can notice a Kelvin response (and a Walker circulation) over the tropical Atlantic, the Venezuelan-Colombian Llanos, and Amazon basins, with easterly winds that travel parallel to the equator heating source, where the winds ascend and then return to the Atlantic in the high troposphere. On the west side of the heating source, two cyclones generate strong westerly winds due to a planetary wave response. One is in the northwest, which forces the flow to cross Central America, recurving to northern South America, and there is also another similar recurving from the Peruvian coast. Winds rise on the heat source by a vortex tube that directs the winds poleward in the troposphere's high levels.

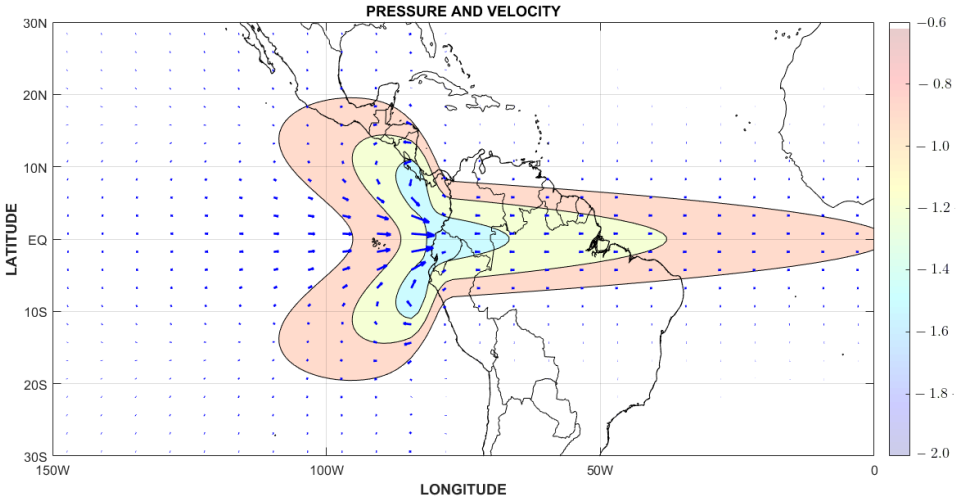

Figure 3. Surface flow (wind arrows) and pressure contours over Northern South America and Meso-America for a diabatic heating source located at the equator ($k = 4$, $a = 5$, $I = 1$ and $y_0 = 0$).

Using this classical Matsuno-Gill model, we could integrate the previous analysis of the atmospheric circulation over northern South America into a single physical framework. Among other things, this theoretical framework provides: (i) An explanation for the recurving winds coming from the Caribbean sea (no satisfactory description until now). (ii) A reinterpretation of the re-curvature of the winds coming from the Peruvian coasts (the called CHOCO Jet) using a new argument not related to the Stensrud mechanisms. (iii) A connection between (i) and (ii) with the existence of a Walker cell between the tropical Atlantic, Northern South America, and far Eastern Pacific.

2.2. Response to an Asymmetric Location of the Diabatic Heating Source

The heating source is at the equator only near boreal spring, so it is necessary to bring a more realistic heat source location at about 5° N. Figure 4 shows the diabatic heating source (red) and its meridional components. The diabatic heating's asymmetric place forces the first six harmonics confined within the tropics. According to the spectrum, Q_0 excites the Kelvin mode, Q_1 the mixed-mode, and $Q_{n\geq 1}$ the planetary modes. The Kelvin wave drives the dynamics to the east of the source, while the mixed wave is in phase with the heating source and the superposition of planetary waves force the dynamics to the west of the heating source.

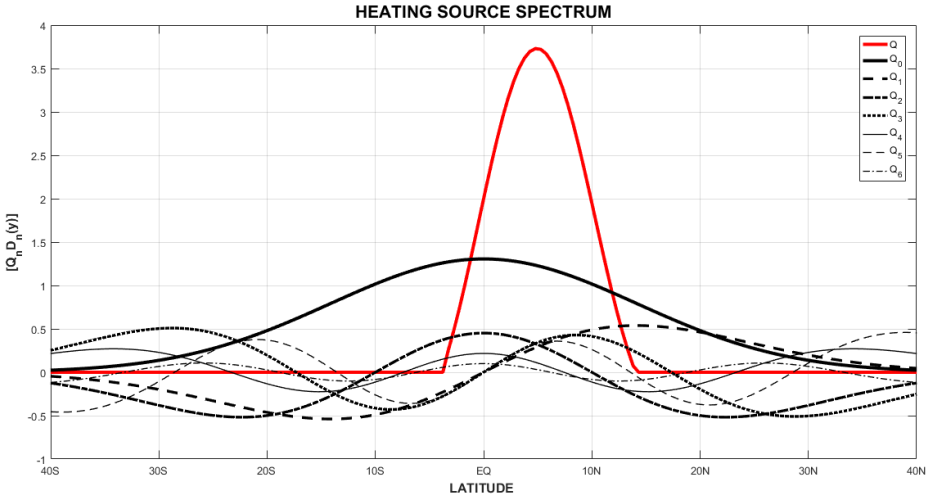

Figure 4. Spectrum of the diabatic heating source located at 5°N (**red**) and its meridional components (**black**).

Figure 5 shows the main circulation patterns over Northern South America and Meso-America for a diabatic heating source located at 5° N. Because the heating source is still close to the equator, many of the Kelvin patterns persist. For example, the projection onto $D_0(y)$ remains substantial, so the easterly flow is almost intact, preserving most of Walker's cell features, with a slight reduction in its intensity. The southwest inflow now locates north of the equator. The vortex stretching mechanism becomes more significant than in the symmetric case, and the poleward flow to the north in the heating region increases correspondingly. As the poleward flow increases so - by the geostrophic relation—a low to the west develops [24].

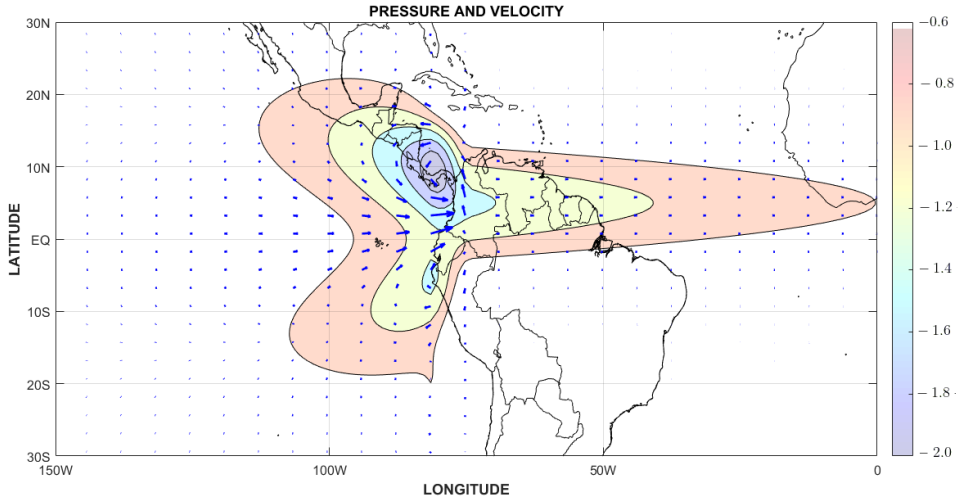

Figure 5. Surface flow (wind arrows) and pressure contours over Northern South America and Meso-America for a diabatic heating source located at 5°N ($k = 4$, $a = 5$, $I = 1$ and $y_0 = 0.5$).

The minimum pressure is found to the west and slightly poleward of the heating maximum because of the planetary waves' superposition. In the case of the diabatic heating source in Colombia at 5° N, both cyclones are still present to the west, but the northwest one is strengthened over Panama while the cyclone to the southwest weakens. For this reason, we can conclude that the asymmetric location of the diabatic heating forces the Panama Low. These changes also generate a slight increase

in the magnitude of the westerly winds (the called CHOCO Jet), a small reduction in vertical velocity over the heating area, and increases the easterly flow above 10° N (the Caribean Jet).

2.3. Ambient Wind Influence

The overall geophysical flow over Northern South America and Meso-America are easterly; for this reason, we assume a uniform mean zonal wind, $\Delta = -0.1$, to perform a non-resting flow experiment as is shown in Figure 6) (see Equation (3) to (5) bellow). The main change is that the amplitude and the planetary waves' decay rate are both considerably reduced [24]; for this reason, the westerly winds weaken. On the other hand, the projection onto the mixed wave allows the northward flow over the heating zone, and easterly winds become more vigorous than for the case of no ambient wind. Finally, it is possible to observe a slight displacement towards the east of the low pressure, which now locates over Colombia at 10° N.

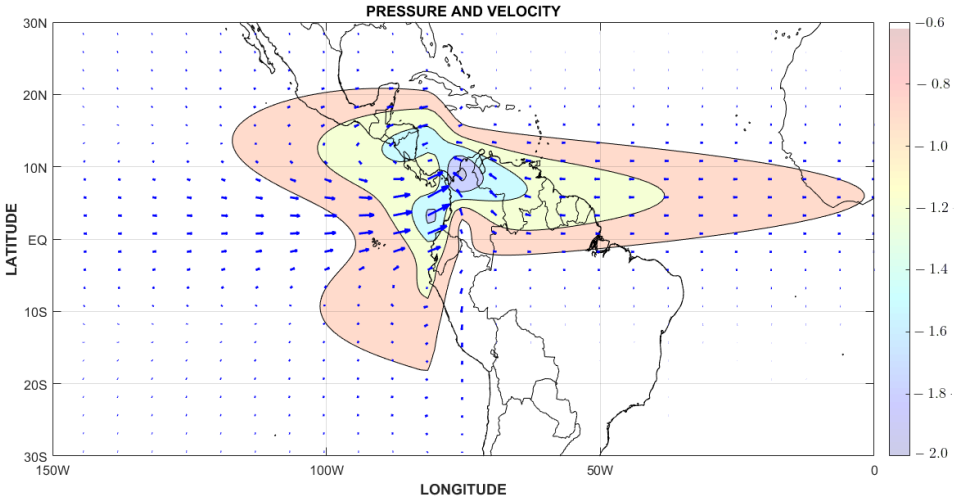

Figure 6. Surface flow (wind arrows) and pressure contours over Northern South America and Meso-America for a diabatic heating source located at 5° N ($k = 4$, $a = 5$, $I = 1$ and $y_0 = 0.5$) in the presence of an ambient easterly wind ($\Delta = -0.1$).

2.4. Mechanism for a Regional Heat-Induced Circulation

Using the results of Section 2.1, one can propose a conceptual scheme about the general circulation in the low (850 hPa) and high (300 hPa) troposphere over northern South America and Meso-America (see Figure 7) consisting of a Rossby-Kelvin pattern along the lines of the Matsuno-Gill concept. This pattern matches the observations of Section 1, giving a new qualitative explanation.

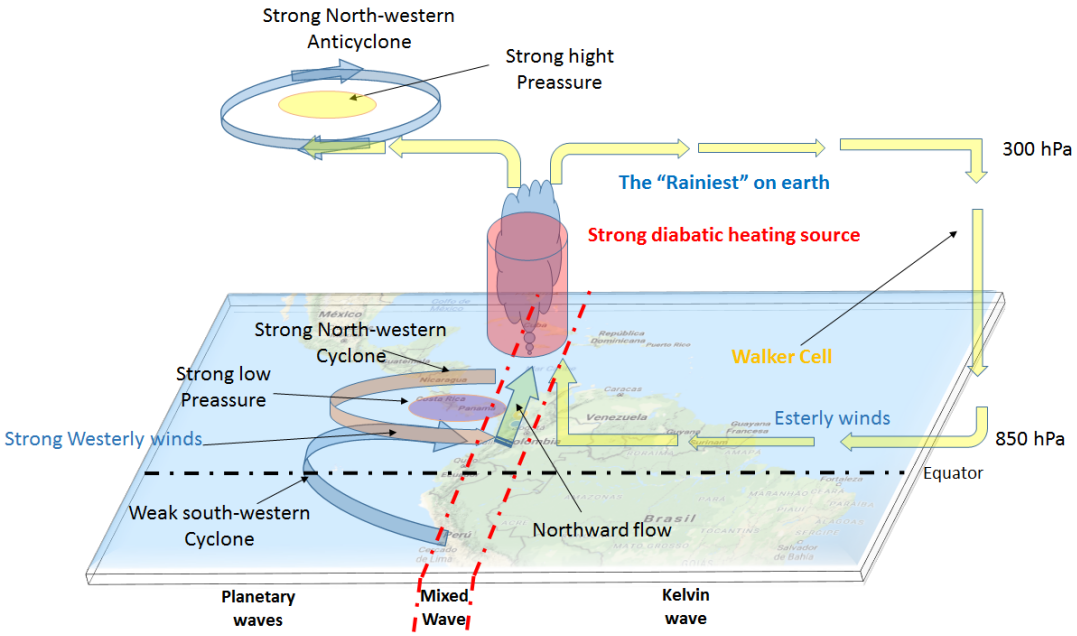

Figure 7. Conceptual scheme of the large scale circulation in northern South America and Meso-America from mid-March to mid-December according to the Matsuno-Gill Response.

3. Discussion

3.1. The Rossby-Kelvin Pattern from Matsuno-Gill Model Matches with the Main Features of Northern South America and Meso-America Circulation

The Heat-Induced Tropical Circulations model proposed by Matsuno-Gill represents a physical explanation of the atmosphere's general circulation in northern South America and Meso-America. This simple conceptual model establishes a paradigm for understanding hydro-climatology in the western hemisphere's tropical region.

A sizeable diabatic heating source over western Colombia is the driver of the circulation in northern South America and Meso-America from mid-March to mid-December. The flow is pervasively forced (everywhere). The planetary and Kelvin waves are "characteristics" or "caustics", creating information pathways that, in turn, dominates the low and upper-level winds fields.

This heating source carries information to the west through a half planetary wave, generating two cyclones responsible for the strong westerly winds. This wave is an excellent feedback example between westerlies and latent heating release on west-facing mountain slopes. To the east of the heating source, a Kelvin wave transmits the information producing a Walker type circulation responsible for the easterly winds coming to northern South America and far eastern Pacific from the east. Under this Rossby-Kelvin Pattern, winds from the Caribbean Sea and the Peruvian coast curve towards Colombia give rise to Earth's rainiest region on the Colombian Pacific coast. Since heating sources drive westerlies, this feedback process is inevitable.

On the other hand, the equatorially asymmetrical location of the diabatic heating (5°) increases the north-western cyclone's magnitude, and the low-level pressure over Panama becomes more potent than in the symmetrical heating case. For this reason, we can conclude that the diabatic heating forces the "Panama Low". Mathematically there should be a vortex tube around the heating source. Finally, the pure barocline mode shows a strong anticyclone in Meso-America, following the observations.

In turn, this circulation pattern feeds back, developing the convection, ascend, condensation, latent heat release, and, therefore, the diabatic heating to start over again.

3.2. Next Task: To Extend This Explanation to Different Time Scales

Linearization simulates observed wave structure reasonably well for this case. A main simplification is that the waves are decoupled from each other. As a consequence, the mutual coupling between the various scales of motion due to turbulence seriously limit the validity of linearization. Therefore, the applications of the results of this linearization are restricted to prognosis studies. However, various applications show that the results are meaningful for the approximately steady-state behaviour of cuasi periodic disturbances [27].

This new qualitatively explanation of northern South America and Meso-America hydro-climatology is remarkable. The physical principles of a heat-induced circulation could apply to different time scales of the geophysical fluid dynamics under the steady-state hypothesis (from the weekly time scale, through the intra-annual, the inter-annual, and climate change). Besides, the linear approximation is a powerful concept. In essence, it allows superposition, positive and negative sources, and time dependence. The superposition principle of linear systems allows decomposition of the circulation to improve the understanding of the relation between the regional circulation and other meteorological and climatic processes. Nevertheless, for prognostic models, one needs to close the feedback cycle between the circulation and the diabatic heating.

An obvious next step is to introduce the Andes as a reflective barrier to these waves, following the method used in [28].

4. Materials and Methods

4.1. Data

Monthly precipitation data in Northern South America are from the Colombian National Institute of hydrology meteorology and environmental studies -IDEAM- data portal (http://dhime.ideam.gov.co/atencionciudadano). We analyze these data from 1960 to 2018 in comparisons with the Reanalysis of monthly precipitation fields presented by [25]. The annual-mean column-integrated heating over the far eastern Pacific, Northern South American, and the Meso-America (40–100 W, 20N–25 S) are from ECMWF ERA-40 Atlas [26]. The horizontal and vertical wind fields are from the European Center for Medium-range Weather Forecasting (ECMWF) ERA-Interim reanalysis data [29]. This data set has the best approximates the climatic and orographic characteristics of northern South America compared to other re-analyzes ([3,30,31]). We use a 0.75° resolution in both longitude and latitude, and monthly data from January-1980 to December 2019.

4.2. Methods

4.2.1. Drawing the Main Features of Heat-Induced Circulation

Following [23], we decompose the heat-induced circulation into their main components. (i) A large amount of precipitation creates a diabatic heating source due to condensation. (ii) diabatic heating is available to influence the surroundings through equatorially trapped waves. (iii) equatorially trapped waves are "characteristics", the large scale circulation follows the pathways traced by those waves, (iv) the feedback is inevitable. The large-scale circulation is responsible for a large amount of precipitation.

To show all those components in northern South America and Meso-America circulation, we draw (a) Annual precipitation map that shows regions with values above 4000 mm/year, for observations, Lopez de Micay (77°14′ W, 2°50′ N) rain gauge station serve as a proxy of maximum precipitation in the area. (b) Total column vertically integrated heating makes evident the great diabatic heating source in northern South America. (c) the streamlines at 850 hPa and 300 hPa levels, and the vertical velocity show the circulation's main patterns. These streamlines exhibit the main features of equatorially trapped waves. A vertical profile of the circulation around 5° N (d) illustrates the Atlantic South

America Walker circulation. For further physical explanation, we used the multi-annual mean for each Figure, assuming a steady-state.

4.2.2. Idealized Model

The Matsuno-Gill model consists of the linear damped shallow-water equation model on an equatorial β plane that provided elegant analytical solutions for some particular heating distributions in steady-state. Its simplicity stems from assuming a purely baroclinic vertical structure, corresponding to a heat source (or sink) at the mid-troposphere [32].

To write the shallow water equations in a non-dimensional form, we define the units of time and length as

$$T = (2\beta c)^{-1/2}, \tag{1}$$

$$a = (c/2\beta)^{1/2}, \tag{2}$$

where a is the equatorial Rossby Radius, and T is a length of time. Here, $c = (gH)^{1/2}$ is the speed of long internal gravity waves ($\sim$60 ms^{-1}) from the equivalent mean layer depth H. When the equivalent depth H is 400 m, the Rossby radius is about 10°, this small size of the Rossby radius justifies the beta-approximation.

Gill introduced dissipative processes using Rayleigh friction and Newtonian cooling. An even more considerable mathematical simplification comes from assuming that those damping mechanisms adopt the same value ε in all the equations. It means that ε represents friction in the momentum equation and cooling in the continuity equation. Using Gill's model formulation by [24], the linearized governing equations, for a non-resting atmosphere with uniform mean zonal wind Δ, are

$$\left(\Delta\frac{\partial}{\partial x} + \varepsilon\right) q + \frac{\partial q}{\partial x} + \left(\frac{\partial}{\partial y} - \frac{1}{2}y\right) v = -Q, \tag{3}$$

$$\left(\Delta\frac{\partial}{\partial x} + \varepsilon\right) r - \frac{\partial r}{\partial x} + \left(\frac{\partial}{\partial y} + \frac{1}{2}y\right) v = -Q, \tag{4}$$

$$2\left(\Delta\frac{\partial}{\partial x} + \varepsilon\right) v + \left(\frac{\partial}{\partial y} + \frac{1}{2}y\right) q + \left(\frac{\partial}{\partial y} - \frac{1}{2}y\right) r = 0. \tag{5}$$

A buoyancy source Q (positive for heating) forces the dynamics. In these equations $q = \phi + u$ and $r = \phi + u$, where (u, v) are the non-dimensional zonal and meridional velocity, respectively, and ϕ is the non-dimensional geopotential perturbation associated with a downward gravitational acceleration g acting on a free-surface height perturbation h. The coordinate (x, y) refers to a non-dimensional distance with x measured eastward and y measured northward from the equator. Δ is the zonal ambient wind. $\Delta = 0$ represents the resting atmosphere case studied in [21].

Equations (3)–(5) have solutions in terms of meridional normal modes with the structure

$$q = q_{n+1}(x,t)\, D_{n+1}(y), \qquad v = v_n(x,t)\, D_n(y), \qquad r = r_{n-1}(x,t)\, D_{n-1}(y), \tag{6}$$

where $D_n(y)$ are the Hermite-Weber or parabolic cylinder functions [33]. These functions satisfy the relationships

$$\frac{\mathrm{d}D_n}{\mathrm{d}y} + \frac{1}{2}yD_n = nD_{n-1}, \qquad \frac{\mathrm{d}D_n}{\mathrm{d}y} - \frac{1}{2}yD_n = -D_{n+1}. \tag{7}$$

The horizontal distribution of the heating source Q is taken to be separable and of the form

$$Q(x,y) = F(x)\sum_{n=0}^{\infty} Q_n D_n(y), \tag{8}$$

whose expansion in terms of parabolic cylindrical functions is

$$Q(x,y) = I\alpha k \sin(kx) D_0\left(\alpha\left(y-y_0\right)\right), \qquad 0 \le x \le \pi/k. \tag{9}$$

where I is the total amount of heat, α, the width of the heating region, π/k, the length of the heating region, and y_0 the latitude of maximum heating. $D_0\left(\alpha\left(y-y_0\right)\right)$ can be expressed as a series in $D_n\left(y\right)$ [24]

$$D_0\left(\alpha\left(y-y_0\right)\right) = \sum_{n=0}^{\infty} d_n D_n(y), \tag{10}$$

where

$$d_0 = \left(\frac{2}{1+\alpha^2}\right)^{\frac{1}{2}} exp\left(-\frac{1}{4}\frac{\alpha^2}{1+\alpha^2}\right), \quad d_{n+1} = \frac{1}{n+1}\left[\left(\frac{1-\alpha^2}{1+\alpha^2}\right) d_{n-1} + \left(\frac{\alpha^2}{1+\alpha^2}\right) y_0 d_n\right]. \tag{11}$$

The heating function can thus be written in the separable form (8), where we take

$$F(x) = k\sin(kx), \qquad Q_n = I\alpha d_n, \qquad 0 \le x \le \pi/k. \tag{12}$$

We can now use Equations (6)–(8) in (3)–(5) to obtain the equations for all the modes:

(i) The Kelvin mode $(n = -1)$. In Equation (6) the lowest value for n is -1, in which case $u = r = 0$. This mode, conventionally called the Kelvin mode, is governed by the single equation

$$\left(\Delta\frac{\partial}{\partial x} + \varepsilon\right) q_0 + \frac{\partial q_0}{\partial x} = -Q_0 F(x). \tag{13}$$

(ii) The mixed mode $(n = 0)$. With $n = 0$ in Equation (6) we have q, $u \neq 0$, $r = 0$, and the equations are

$$\left(\Delta\frac{\partial}{\partial x} + \varepsilon\right) q_1 + \frac{\partial q_1}{\partial x} - v_0 = -Q_1 F(x), \tag{14}$$

$$2\left(\Delta\frac{\partial}{\partial x} + \varepsilon\right) v_0 + q_1 = 0. \tag{15}$$

(iii) Gravity-planetary modes $(n \ge 1)$. Now q, u and r are all non-zero, and the equations are

$$\left(\Delta\frac{\partial}{\partial x} + \varepsilon\right) q_{n+1} + \frac{\partial q_{n+1}}{\partial x} - v_n = -Q_{n+1} F(x), \tag{16}$$

$$\left(\Delta\frac{\partial}{\partial x} + \varepsilon\right) r_{n-1} - \frac{\partial r_{n-1}}{\partial x} + n v_n = -Q_{n-1}(F(x), \tag{17}$$

$$2\left(\Delta\frac{\partial}{\partial x} + \varepsilon\right) v_n + (n+1) q_{n+1} - r_{n-1} = 0. \tag{18}$$

The forced and free solutions for each mode exited can be computed by using the analytical framework presented in [24] or [34].

4.2.3. Theoretical Experiments

One of the advantages of the Phlips and Gill formulation is the possibility of fitting the heating source geometry to local conditions by varying its width, length, and intensity. Furthermore, the analytical solution exposed by Phlips and Gill explains the flow variations in terms of the natural modes, planetary, Kelvin, and gravity-planetary waves, even considering the presence of a mean zonal

wind. For these reasons, we propose the next idealized model experiments to review the main patterns of the heat-induced circulation over northern South America and Meso-America.

The intense diabatic heating source over Colombia is so close to the equator. For that reason, the first model experiment reproduces the heat-induced circulation for an isolated heating region symmetric about the equator at 79°W. in this case, we consider geometry parameters $k = 4$ and $a = 5$ and $y_0 = 0$. Its investigation allows the first draft of the leading regional flow patterns without considering zonal mean flow. The second theoretical experiment studies an isolated heating region off of the equator following diabatic heating source location in Colombia, as is shown in Figure 2b (77° W, 5° N). We also assume $k = 4$ and $a = 5$ and define $y_0 = 0.5$ to shape the diabatic heating geometry with the observations in Figure 2a. Finally, the third experiment includes a zonal mean wind assuming $\Delta = -0.1$ ($\sim$6 ms^{-1} easterly). For diagnosis purposes, $I = 1$ in all cases.

Author Contributions: Conceptualization, methodology, software, validation, and formal analysis, Ó.J.M. and J.D.R.H.; writing—original draft preparation, J.D.R.H.; writing—review and editing, Ó.J.M.; visualization, J.D.R.H.; supervision, Ó.J.M.; project administration, Ó.J.M.; All authors have read and agreed to the published version of the manuscript.

Funding: This research received no external funding, support from a fellowship of the National University to outstanding students is appreciated by J.D.R.H.

Acknowledgments: Data from the Colombian meteorological service, IDEAM, is appreciated.

Conflicts of Interest: The authors declare no conflict of interest.

References

1. Poveda, G.; Waylen, P.R.; Pulwarty, R.S. Annual and inter-annual variability of the present climate in northern South America and southern Mesoamerica. *Palaeogeogr. Palaeoclimatol. Palaeoecol.* **2006**, *234*, 3–27. [CrossRef]
2. Poveda, G.; Jaramillo, L.; Vallejo, L.F. Seasonal precipitation patterns along pathways of South American low-level jets and aerial rivers. *Water Resour. Res.* **2014**, *50*, 98–118. [CrossRef]
3. Arias, P.A.; Martínez, J.A.; Vieira, S.C. Moisture sources to the 2010–2012 anomalous wet season in northern South America. *Clim. Dyn.* **2015**, *45*, 2861–2884. [CrossRef]
4. Poveda, G.; Mesa, O.J. On the existence of Lloró (the rainiest locality on Earth): Enhanced ocean-land-atmosphere interaction by a low-level jet. *Geophys. Res. Lett.* **2000**, *27*, 1675–1678. [CrossRef]
5. Ahrens, C.D. *Essentials of Meteorology: An Introduction to the Atmosphere*, 2nd ed.; Wadsworth: Belmont, CA, USA, 1998.
6. Xie, S.P.; Xu, H.; Saji, N.; Wang, Y.; Liu, W.T. Role of narrow mountains in large-scale organization of Asian monsoon convection. *J. Clim.* **2006**, *19*, 3420–3429. [CrossRef]
7. Chan, S.C.; Nigam, S. Residual diagnosis of diabatic heating from ERA-40 and NCEP reanalyses: Intercomparisons with TRMM. *J. Clim.* **2009**, *22*, 414–428. [CrossRef]
8. Zhang, K.; Randel, W.J.; Fu, R. Relationships between outgoing longwave radiation and diabatic heating in reanalyses. *Clim. Dyn.* **2017**, *49*, 2911–2929. [CrossRef]
9. Serra, Y.L.; Kiladis, G.N.; Hodges, K.I. Tracking and mean structure of easterly waves over the Intra-Americas Sea. *J. Clim.* **2010**, *23*, 4823–4840. [CrossRef]
10. Stensrud, D.J. Importance of Low-Level Jets to Climate: A Review. *J. Clim.* **1996**, *9*, 1698–1711. [CrossRef]
11. Bjerknes, J. Atmospheric teleconnections from the equatorial Pacific. *Mon. Wea. Rev* **1969**, *97*, 163–172. [CrossRef]
12. Krishnamurti, T. Tropical east-west circulations during the northern summer. *J. Atmos. Sci.* **1971**, *28*, 1342–1347. [CrossRef]
13. Krishnamurti, T.; Kanamitsu, M.; Koss, W.J.; Lee, J.D. Tropical east–west circulations during the northern winter. *J. Atmos. Sci.* **1973**, *30*, 780–787. [CrossRef]
14. Trenberth, K.E.; Stepaniak, D.P.; Caron, J.M. The global monsoon as seen through the divergent atmospheric circulation. *J. Clim.* **2000**, *13*, 3969–3993. [CrossRef]
15. Webster, P.J. The large-scale structure of the tropical atmosphere. In *Large-Scale Dynamical Processes in the Atmosphere*; Cambridge University Press: Cambridge, UK, 2001; p. 235.

16. Lau, K.; Yang, S. Walker circulation. *Encycl. Atmos. Sci.* **2003**, 2505–2510.
17. Stechmann, S.N.; Ogrosky, H.R. The Walker circulation, diabatic heating, and outgoing longwave radiation. *Geophys. Res. Lett.* **2014**, *41*, 9097–9105. [CrossRef]
18. Wang, C. Atlantic climate variability and its associated atmospheric circulation cells. *J. Clim.* **2002**, *15*, 1516–1536. [CrossRef]
19. Wang, C. ENSO, Atlantic climate variability, and the Walker and Hadley circulations. In *The Hadley Circulation: Present, Past and Future*; Springer: Berlin/Heidelberg, Germany, 2004; pp. 173–202.
20. Webster, P.J. Response of the tropical atmosphere to local, steady forcing. *Mon. Wea. Rev.* **1972**, *100*, 518–541. [CrossRef]
21. Gill, A.E. Some simple solutions for heat-induced tropical circulation. *Q. J. R. Meteorol. Soc.* **1980**, *106*, 447–462. [CrossRef]
22. Matsuno, T. Quasi-geostrophic motions in the equatorial area. *J. Meteorol. Soc. Japan. Ser. II* **1966**, *44*, 25–43. [CrossRef]
23. Holton, J.R.; Hakim, G.J. *An Introduction to Dynamic Meteorology*; Academic Press: Cambridge, MA, USA , 2012; Volume 88.
24. Phlips, P.; Gill, A. An analytic model of the heat-induced tropical circulation in the presence of a mean wind. *Q. J. R. Meteorol. Soc.* **1987**, *113*, 213–236. [CrossRef]
25. Hurtado-Montoya, A.F.; Mesa, Ó.J. Reanalysis of monthly precipitation fields in Colombian territory. *Dyna* **2014**, *81*, 251–258. [CrossRef]
26. Kållberg, P.; Berrisford, P.; Hoskins, B.; Simmons, A.; Lamy-thépaut, S.; Hine, R. *ERA-40 Atlas*; ECMWF: Shinfield Park, Reading, UK, 2005.
27. Volland, H. *Atmospheric Tidal and Planetary Waves*; Springer Science & Business Medi: Berlin, Germany, 2012; Volume 12.
28. Anderson, D.L. The low-level jet as a western boundary current. *Mon. Weather Rev.* **1976**, *104*, 907–921. [CrossRef]
29. Dee, D.P.; Uppala, S.M.; Simmons, A.; Berrisford, P.; Poli, P.; Kobayashi, S.; Andrae, U.; Balmaseda, M.; Balsamo, G.; Bauer, d.P.; et al. The ERA-Interim reanalysis: Configuration and performance of the data assimilation system. *Q. J. R. Meteorol. Soc.* **2011**, *137*, 553–597. [CrossRef]
30. Hoyos, I.; Baquero-Bernal, A.; Hagemann, S. How accurately are climatological characteristics and surface water and energy balances represented for the Colombian Caribbean Catchment Basin? *Clim. Dyn.* **2013**, *41*, 1269–1290. [CrossRef]
31. Hoyos, I.; Dominguez, F.; Cañón-Barriga, J.; Martínez, J.; Nieto, R.; Gimeno, L.; Dirmeyer, P. Moisture origin and transport processes in Colombia, northern South America. *Clim. Dyn.* **2018**, *50*, 971–990. [CrossRef]
32. Davey, M.; Gill, A. Experiments on tropical circulation with a simple moist model. *Q. J. R. Meteorol. Soc.* **1987**, *113*, 1237–1269. [CrossRef]
33. Abramowitz, M. *Handbook of Mathematical Functions*; Number 55 in Applied Mathematics Series, National Bureau of Standards; U.S. Government Printing Office: Washington, DC, USA, 1964.
34. Dalu, G.A.; Gaetani, M.; Lavaysse, C.; Flamant, C.; Evan, A.T.; Baldi, M. Simple solutions for the summer shallow atmospheric circulation over North Africa. *Q. J. R. Meteorol. Soc.* **2018**, *144*, 765–779. [CrossRef]